

Variational theory of multicomponent quantum fluids: An application to positron-electron plasmas at $T=0$

Lauri J. Lantto*

Department of Physics, University of Tennessee, Knoxville, Tennessee 37996-1200

(Received 13 April 1987)

Variational many-body theory is employed to study ground-state properties of hypothetical positron-electron plasmas. We make use of the multicomponent Fermi hypernetted-chain method to calculate the energy and pair-correlation functions of this system. Optimization of the trial wave function is performed through solving a set of approximate Euler-Lagrange equations for the pair distribution functions. Electron densities are chosen to be in the metallic range, and several concentrations of positrons are considered. At fifty-fifty concentration this system represents an idealized model of the electron-hole liquid and at the limit of zero concentration we have a single positron impurity in an electron gas. Results of this work support earlier theoretical predictions for the model electron-hole liquid and are in good agreement with available experimental evidence for both the electron-hole liquid and the single positron impurity.

I. INTRODUCTION

Ground-state properties of a variety of quantum fluids have been studied by means of variational many-body theory. Systems of interest range from the electron gas¹ to high-density helium liquids² and nuclear matter.³ Boson and fermion fluids including binary mixtures,⁴⁻⁶ mostly homogeneous infinite matter, but recently inhomogeneous surfaces^{7,8} have also been investigated. A common factor in many of these systems is a strong two-body interaction which requires special treatment if perturbation theory is applied. Selected graphical contributions have to be summed to infinite order. Much of the success of the variational method is based on the fact that it is capable of handling simultaneously both strong short-range and long-range correlations between two particles in the medium. In terms of perturbation theory, this means that both ladder- and ring-diagram contributions are incorporated in the variational wave function,⁹ at least in some sensible approximation. This is achieved by employing hypernetted-chain integral-equation techniques and Euler-Lagrange equations to optimize the trial wave function and to calculate the energy and correlation functions of the system under consideration.

In this work we present the Fermi hypernetted-chain (FHNC) method for multicomponent fluids and derive a set of approximate Euler-Lagrange (EL) equations for the partial pair distribution (pair-correlation) functions of such systems. Then we apply these techniques to compute ground-state quantities for a hypothetical electron-positron mixture. We consider the metallic range of electron densities and several concentrations of positrons. At 50% concentration this two-component plasma represents an idealized model¹⁰ for the electron-hole liquid found in some semiconductors. At other concentrations of positrons, the energies and pair-correlation functions of this system may be used to fabri-

cate the energy functional for two-component density-functional theory.¹¹ Finally, in the limit of zero concentration we calculate the energy and the annihilation rate of a positron impurity in the electron gas.

The plan of the paper is following. In Sec. II we present the multicomponent FHNC equations in the form suitable for later use in Sec. III, where EL equations for partial pair-correlation functions are derived. The special case of an impurity particle in the electron fluid is treated in Sec. IV and, finally, Sec. V is devoted to results and discussion.

II. MULTICOMPONENT FERMION HYPERNETTED-CHAIN EQUATIONS

In this section we present the FHNC equations for homogeneous many-component liquids and use them to obtain a simple expression for the variational ground-state energy. We consider a model of n interpenetrating fluids, each of which consists of N_α ($\alpha=1,2,\dots,n$) particles in a common volume V , at zero temperature, such that all the partial densities $\rho_\alpha=N_\alpha/V$ remain constant as N_α and V go to infinity. The ground-state wave function for such a multicomponent system is approximated by a variational trial function of standard form

$$\Psi = \prod_{\substack{\alpha,\beta=1 \\ \alpha \leq \beta}}^n F_{\alpha\beta} \left[\prod_{\alpha=1}^n \phi_\alpha \right]. \quad (1)$$

Here each ϕ_α is the many-body wave function of N_α noninteracting particles of species α , i.e., a Slater determinant of single-particle states for fermions and a constant for bosons. Pairwise correlations are built into the many-body wave function through

$$F_{\alpha\beta} = \prod_{i,j} f_{\alpha\beta}(\mathbf{r}_{\alpha i}, \mathbf{r}_{\beta j}), \quad (2)$$

where $i=1,\dots,N_\alpha$, $j=1,\dots,N_\beta$ for $\alpha \neq \beta$ and

$i = 1, \dots, N_\alpha - 1, j = 2, \dots, N_\alpha$ for $\alpha = \beta$, such that each pair of particles appears only once in this product. In the case of a two-component fluid, for example, we have two Slater determinants (which are known) and three correlation factors f_{11}, f_{12} , and f_{22} which have to be determined by optimizing the energy of the system. The FHNC integral equations allow us to calculate pair-correlation functions $g_{\alpha\beta}$ and energy corresponding to the wave function (1), if the $f_{\alpha\beta}$ are known. The graphical expansion leading to the FHNC integral equations will not be discussed here; we refer to original works^{12,13} and review articles^{14,15} for background material in this subject and detailed derivation of those equations. In the following, only a brief review of the FHNC theory is given, while the equations are presented in the form suitable for multicomponent systems.

Extension of the FHNC method to many-component systems is straightforward. As in the one-component case, each pair distribution function $g_{\alpha\beta}$ is decomposed into partial contributions

$$g_{\alpha\beta}(\mathbf{r}_{12}) = 1 + \Gamma_{\alpha\beta}^{dd}(\mathbf{r}_{12}) + \Gamma_{\alpha\beta}^{de}(\mathbf{r}_{12}) + \Gamma_{\alpha\beta}^{ed}(\mathbf{r}_{12}) + \Gamma_{\alpha\beta}^{ee}(\mathbf{r}_{12}), \quad (3)$$

where each Γ_{12}^i represents certain subclasses of diagrams labeled by superscript i ($i = dd, de, ed, ee$). The subscripts $\alpha\beta = 11, 12, 22, \dots$ refer to component species α and β . Every $\Gamma_{\alpha\beta}^i$ is further decomposed into sums of nodal ($N_{\alpha\beta}^i$) and non-nodal or direct ($X_{\alpha\beta}^i$) diagrams,

$$\Gamma_{\alpha\beta}^i = N_{\alpha\beta}^i + X_{\alpha\beta}^i. \quad (4)$$

A nodal diagram is such that it can be cut into two disconnected pieces by removing one internal point (node). Hence they may be summed by solving convolution integral equations. In homogeneous systems these convolutions can be conveniently expressed as products in momentum space. Therefore we introduce the dimensionless Fourier transform defined as

$$X_{\alpha\beta}(\mathbf{k}) = (\rho_\alpha \rho_\beta)^{1/2} \int d\mathbf{r} e^{i\mathbf{k}\cdot\mathbf{r}} X_{\alpha\beta}(\mathbf{r}). \quad (5)$$

Now, a simple rule is followed in writing down the convolution equations. Namely, each $N_{\alpha\beta}$ is calculated as a sum of all possible products of $\Gamma_{\alpha\beta}$ and $X_{\alpha\beta}$ which are allowed by the graphical rules of the FHNC expansion. These rules say, for example, that exchange loops in diagrams cannot connect different types of particles and further that those loops must not overlap. This implies that a convolution term like $\Gamma_{\alpha\gamma}^{de} X_{\gamma\beta}^{de}$ contributes to $N_{\alpha\beta}^{de}$, but $\Gamma_{\alpha\gamma}^{de} X_{\gamma\beta}^{ee}$ is not allowed. In the many-component case it is obviously most economical to make use of matrix notation in writing down all these integral equations for every $N_{\alpha\beta}^i$. Hence, in what follows, we use N^i without subscripts to denote the matrix whose matrix elements are $N_{\alpha\beta}^i$, and similarly for $\Gamma_{\alpha\beta}^i$ and $X_{\alpha\beta}^i$. Then the multicomponent FHNC convolutions can be written as a set of matrix equations

$$N^{dd}(\mathbf{k}) = \Gamma^{dd} X^{dd} + \Gamma^{dd} X^{ed} + \Gamma^{de} X^{dd}, \quad (6a)$$

$$N^{de}(\mathbf{k}) = \Gamma^{dd} X^{de} + \Gamma^{dd} X^{ee} + \Gamma^{de} X^{de}, \quad (6b)$$

$$N^{ed}(\mathbf{k}) = \Gamma^{ed} X^{dd} + \Gamma^{ed} X^{ed} + \Gamma^{ee} X^{dd}, \quad (6c)$$

$$N^{ee}(\mathbf{k}) = \Gamma^{ed} X^{de} + \Gamma^{ed} X^{ee} + \Gamma^{ee} X^{de}, \quad (6d)$$

$$N^{cc}(\mathbf{k}) = (\Gamma^{cc} - L) X^{cc}. \quad (6e)$$

Here, L is a diagonal matrix whose elements give the occupation probability of single-particle states of the ideal fermion system, i.e., $L_{\alpha\beta} = \delta_{\alpha\beta}$ if $k < k_{F_\alpha}$ and zero otherwise. For notational economy, we have dropped the argument \mathbf{k} from Γ 's and X 's on the right-hand side (rhs) of these equations. We note that N^{dd} and N^{ee} are symmetric matrices, N^{ed} is a transpose of N^{de} , and N^{cc} is diagonal; thus the actual number of unknown functions is reduced by symmetry. For example, in the two-component case only 12 functions, instead of 20, need be solved. Similar symmetries hold for Γ^i and X^i also. Now, given the "direct correlation" functions $X_{\alpha\beta}^i$, one may iterate Eqs. (6a)–(6e) to construct the chains of these links. The idea of hypernetting the chains means, of course, that the links $X_{\alpha\beta}^i$ depend on chains $N_{\alpha\beta}^i$, and vice versa. This dependence is conveniently given in \mathbf{r} space for the matrix elements on each X^i . First, we observe that

$$\Gamma_{\alpha\beta}^{dd}(\mathbf{r}_{12}) = f_{\alpha\beta}^2(\mathbf{r}_{12}) \exp[N_{\alpha\beta}^{dd}(\mathbf{r}_{12})] - 1. \quad (7)$$

Then the netting of the chains is achieved by writing

$$X_{\alpha\beta}^{dd}(\mathbf{r}_{12}) = \Gamma_{\alpha\beta}^{dd} - 1 - N_{\alpha\beta}^{dd}, \quad (8a)$$

$$X_{\alpha\beta}^{de}(\mathbf{r}_{12}) = \Gamma_{\alpha\beta}^{dd} N_{\alpha\beta}^{de}, \quad (8b)$$

$$X_{\alpha\beta}^{ee}(\mathbf{r}_{12}) = \Gamma_{\alpha\beta}^{dd} N_{\alpha\beta}^{ee} + (1 + \Gamma_{\alpha\beta}^{dd}) \times [N_{\alpha\beta}^{ed} N_{\alpha\beta}^{de} - \nu_\alpha (N_{\alpha\beta}^{cc} - L_{\alpha\beta})^2], \quad (8c)$$

$$X_{\alpha\beta}^{cc}(\mathbf{r}_{12}) = \Gamma_{\alpha\beta}^{dd} (N_{\alpha\beta}^{cc} - L_{\alpha\beta}). \quad (8d)$$

Here again we suppressed the argument \mathbf{r}_{12} on the rhs of Eqs. (8a)–(8d). For each $X_{\alpha\beta}^i$ the rhs represents the most general diagram constructed of a single link and chains of it, compatible with graphical rules, such that it has two external points (\mathbf{r}_1 and \mathbf{r}_2) and no internal nodes. (We ignore so-called elementary diagrams, except the single link.) For example, one may exponentiate dd -type chains, but not those of type ed or ee because the exchange loops must not overlap. Note that N^{cc} and L are diagonal; in \mathbf{r} space $L_{\alpha\beta}$ represents the one-body density matrix of the noninteracting Fermion fluid, i.e., the single-particle plane-wave states lead to

$$L_{\alpha\beta}(\mathbf{r}) = \delta_{\alpha\beta} l(k_{F_\alpha} \mathbf{r}) / \nu_\alpha, \quad (9)$$

where $l(x) = 3j_1(x)/x$ and ν_α is the degeneracy of species α . If the correlation factors $f_{\alpha\beta}$ are known, the FHNC equations (6a)–(6e) and (8a)–(8d) can be solved, perhaps by a straightforward iteration, to obtain the pair-correlation functions $g_{\alpha\beta}$. However, we wish to invert them in such a way that they can be solved for $f_{\alpha\beta}$ assuming that the $g_{\alpha\beta}$ are known. This allows us to compute the energy for a given set of the $g_{\alpha\beta}$. To reach that goal we calculate $\Gamma_{\alpha\beta}^{dd}$ appearing in Eqs. (8b)–(8d) using the following \mathbf{r} -space relation:

$$1 + \Gamma_{\alpha\beta}^{dd}(\mathbf{r}) = g_{\alpha\beta} / [1 + N_{\alpha\beta}^{de} + N_{\alpha\beta}^{ed} + N_{\alpha\beta}^{de} N_{\alpha\beta}^{ed} + N_{\alpha\beta}^{ee} - \nu_\alpha (N_{\alpha\beta}^{cc} - L_{\alpha\beta})^2]. \quad (10)$$

To simplify the notation, we introduce two matrices,

$$b(\mathbf{k}) = [I + X^{ee}(\mathbf{k})]^{-1}, \quad (11a)$$

$$c(\mathbf{k}) = I - X^{de}(\mathbf{k}), \quad (11b)$$

and define the matrix of structure functions

$$[S(\mathbf{k}) - I]_{\alpha\beta} = (\rho_\alpha \rho_\beta)^{1/2} \int d\mathbf{r} e^{i\mathbf{k}\cdot\mathbf{r}} [g_{\alpha\beta}(\mathbf{r}) - 1]. \quad (12)$$

Then we are ready to solve $N_{\alpha\beta}^i$ in terms of $X_{\alpha\beta}^i$ and $S_{\alpha\beta}$. After some manipulation of Eqs. (6b)–(6d), we obtain

$$N^{de}(\mathbf{k}) = bc^T S (I - cb) + b - I - X^{de}, \quad (13a)$$

$$N^{ee}(\mathbf{k}) = bc^T S cb + S (I - cb) - bc^T S - b + I - X^{ee}, \quad (13b)$$

$$N^{cc}(\mathbf{k}) = (X^{cc} - L) X^{cc} (I - X)^{-1}. \quad (13c)$$

Here superscript T refers to transposed matrix. Now, these relations, together with Eqs. (8b)–(8d), make up the FHNC equations which we need to solve for any given set of functions $g_{\alpha\beta}$. For two-component fluids, only nine $N_{\alpha\beta}^i$ and $X_{\alpha\beta}^i$ need be solved, because N^{ee} is symmetric and N^{cc} is diagonal. In practice, we solve these equations by iteration.

Once the above set of the FHNC equations is solved, we may proceed to the energy calculation. The total energy of a multicomponent fluid described by the wave function (1) may be written in the FHNC approximation as

$$\begin{aligned} \frac{E}{V} = & \sum_{\alpha,\beta} \frac{1}{2} \rho_\alpha \rho_\beta \int d\mathbf{r} \left[g_{\alpha\beta}(\mathbf{r}) v_{\alpha\beta}(\mathbf{r}) - \frac{\hbar^2}{8\mu_{\alpha\beta}} g_{\alpha\beta}(\mathbf{r}) \nabla^2 \{ \ln[1 + \Gamma_{\alpha\beta}^{dd}(\mathbf{r})] - N_{\alpha\beta}^{dd}(\mathbf{r}) \} \right] \\ & - \sum_{\alpha} v_{\alpha\alpha} \rho_\alpha^2 \frac{\hbar^2}{4m_\alpha} \int d\mathbf{r} \{ \Gamma_{\alpha\alpha}^{dd}(\mathbf{r}) [\nabla^2 L_\alpha^2(\mathbf{r}) - 2N_{\alpha\alpha}^{cc}(\mathbf{r}) \nabla^2 L_\alpha(\mathbf{r})] \}. \end{aligned} \quad (14)$$

Here, $v_{\alpha\beta}$ is the potential between a pair of particles and $\mu_{\alpha\beta}$ is their reduced mass. In order to calculate $\Gamma_{\alpha\beta}^{dd}$ and $N_{\alpha\beta}^{dd}$ we make use of the FHNC equations to obtain (matrix) relations

$$\Gamma^{dd}(\mathbf{k}) = bc^T S cb - b, \quad (15)$$

$$X^{dd}(\mathbf{k}) = cbc^T - S^{-1}, \quad (16)$$

and observe that $N^{dd} = \Gamma^{dd} - X^{dd}$. In writing Eq. (14) we have, for simplicity, ignored one (three-body) term which belongs to the full FHNC energy expression.¹⁶ However, that term is usually very small and may be safely neglected, except at the highest densities. Comparable or larger contributions to energy may be missing due to the fact that we have omitted so-called elementary diagrams from the FHNC expansion. Also, the wave function (1) could be improved by including, for example, explicit three-body correlations into it. Calculation of elementary diagrams is not practical, but, unfortunately, their contributions cannot be totally ignored. Namely, an exact property of the quantities $X_{\alpha\beta}^{de}(\mathbf{k})$ is that they should vanish in the small- k limit,^{17,1} but in the present FHNC approximation this property is not satisfied. In applications to be described below, we shall impose such condition in a simple manner, which also may affect the energy by an amount comparable to the omitted three-body correlations. It may be that these neglected contributions cancel each other, to some extent at least, but clearly the energy expression (14) is not exact and therefore we do not attempt to optimize it exactly. Instead, an approximate optimization of it by means of Euler-Lagrange equations is discussed in the next section.

III. OPTIMIZATION OF THE TRIAL WAVE FUNCTION

Earlier we presented a practical method^{18–20} for optimization of the FHNC energy of a one-component

fluid. In that method the quantities N^i and X^i were treated as variables, in addition to $g(\mathbf{r})$, with respect to which the energy was minimized, and the FHNC equations were treated as constraints to be handled by means of Lagrange multipliers. Extending such a procedure to multicomponent systems would be straightforward but tedious. Instead of doing that, we simplify matters considerably by deriving and solving approximate EL equations for $g_{\alpha\beta}$. We start by considering a weakly interacting many-component fermion system, or, equivalently, the low-momentum behavior for a strongly correlated system. Then we can make the following low-order approximations: $N^{cc} = 0$, $X^{de} = 0$, and $1 + X^{ee}(\mathbf{k}) = S_F(\mathbf{k})$, which means that

$$c(\mathbf{k}) = I, \quad (17a)$$

$$b(\mathbf{k}) = [S_F(\mathbf{k})]^{-1}. \quad (17b)$$

Here, S_F is a diagonal matrix whose elements are structure functions of the ideal fermion system. In fact, Eqs. (17a) and (17b) represent the correct limiting behavior¹⁷ for $c(\mathbf{k})$ and $b(\mathbf{k})$ as $k \rightarrow 0$, even for strongly correlated systems. From Eq. (15) we see that $\Gamma_{\alpha\beta}^{dd}$ is a long-range quantity, proportional to $1/r^2$ at large r . In weakly correlated systems it is small at short range, too, so that we may expand the logarithm $\ln(1 + \Gamma_{\alpha\beta}^{dd})$ in powers of $\Gamma_{\alpha\beta}^{dd}$ and neglect terms of second and higher order in $\Gamma_{\alpha\beta}^{dd}$. Doing this, the energy expression (14) simplifies so much that we can solve the optimization problem analytically. The result is

$$[S(\mathbf{k})MS(\mathbf{k})]^{-1} = [S_F(\mathbf{k})MS_F(\mathbf{k})]^{-1} + \frac{4}{\hbar^2 k^2} v(\mathbf{k}), \quad (18)$$

where $M = \text{diag}(m_\alpha)$ is a diagonal mass matrix and $v(\mathbf{k})$ is a matrix of the pair potentials in Fourier space. This expression may be used to study the low-momentum behavior of the optimal structure functions for a given po-

tential $v(\mathbf{k})$. In order to go beyond the weakly interacting limit or to improve the treatment of short-range correlations, we note that

$$\ln(1 + \Gamma_{\alpha\beta}^{dd}) - N_{\alpha\beta}^{dd} = \ln g_{\alpha\beta} - (g_{\alpha\beta} - 1) + X_{\alpha\beta}^{dd} + \frac{1}{2}[(\Gamma_{\alpha\beta}^{dd})^2 - (g_{\alpha\beta} - 1)^2] + \dots \quad (19)$$

We omit the last term on the rhs of Eq. (19), then insert it into the energy expression (14) and minimize with respect to $g_{\alpha\beta}$ to obtain the following set of EL equations:

$$-\frac{\hbar^2}{2\mu_{\alpha\beta}} \nabla^2 [g_{\alpha\beta}(\mathbf{r})]^{1/2} + [v_{\alpha\beta}(\mathbf{r}) + w_{\alpha\beta}(\mathbf{r})][g_{\alpha\beta}(\mathbf{r})]^{1/2} = 0. \quad (20)$$

Now, the ‘‘induced potentials’’ $w_{\alpha\beta}$ that depend on $g_{\alpha\beta}$ may be conveniently written using matrix notation in \mathbf{k} space,

$$w(\mathbf{k}) = -\frac{\hbar^2 k^2}{4} \{ [S(\mathbf{k})MS(\mathbf{k})]^{-1} - [S_F(\mathbf{k})MS_F(\mathbf{k})]^{-1} + M[S(\mathbf{k}) - 1] + [S(\mathbf{k}) - 1]M \}. \quad (21)$$

Equations (20) and (21) represent a generalization of the one-component FHNC variational EL equations to arbitrary many-component mixture of fermion and/or boson fluids. However, this set of EL equations represents only approximate optimization of the FHNC energy expression, but numerical results to be described below prove that this is a very sensible approximation. Note that in a boson system S_F is to be replaced by a unit matrix; then Eq. (21) leads to $w_{\alpha\beta}$ derived by Chakraborty⁵ for two-component boson mixture. We may write

$$w = w^B + w^{\text{ex}}, \quad (22)$$

where w^B represents a boson system and w^{ex} an additional exchange contribution for fermion fluid. The explicit expression for w^{ex} is seen to be

$$w_{\alpha\beta}^{\text{ex}}(\mathbf{k}) = -\delta_{\alpha\beta} \frac{\hbar^2 k^2}{4m_\alpha} [(1 - S_{F_\alpha}^{-2}(\mathbf{k}))]. \quad (23)$$

Thus the induced exchange potential is diagonal, repulsive, and vanishes for $k > 2k_{F_\alpha}$. This shows that fer-

mions feel an effective induced repulsion due to the antisymmetry of the wave function. Because $w_{\alpha\beta}$ and $g_{\alpha\beta}$ are to be solved self-consistently, the actual difference between the fermion- and boson-induced potentials is not, in general, equal to that given by Eq. (23).

The above set of nonlinear integro-differential equations can be solved numerically by employing a method which is direct generalization of a linearization procedure developed earlier.^{18,5} However, before discussing numerical techniques, we consider a special case of an impurity particle embedded into a fermion fluid.

IV. VARIATIONAL EQUATIONS FOR SINGLE IMPURITY PARTICLE

From the multicomponent formalism discussed above, we may easily derive the FHNC theory for screening and correlation of a mobile impurity particle embedded into an interacting fermion (or boson) fluid. Here we consider only the simplest case of a one-component host, such as the jellium electron gas. Clearly, generalization to the case of many-component host system would be straightforward.

We start from the two-component theory discussed above. Now, subscripts $\alpha=1$ and $\beta=2$ are used to refer to the host and impurity particles, respectively. In the many-body wave function (1) we set $N_2=1$, $F_{22}=1$, and $\phi_2=1$. Thus only f_{11} and f_{21} , or, equivalently, g_{11} and g_{21} remain unknown, and $g_{22}=1$. Now, g_{21} can be expressed as

$$g_{21}(\mathbf{r}) = 1 + \Gamma_{21}^{dd}(\mathbf{r}) + \Gamma_{21}^{de}(\mathbf{r}), \quad (24)$$

and for a given g_{21} we calculate Γ_{21}^{dd} using

$$1 + \Gamma_{21}^{dd}(\mathbf{r}) = g_{21}(\mathbf{r}) / [1 + N_{21}^{de}(\mathbf{r})]. \quad (25)$$

In order to derive the FHNC equations for N_{21}^{de} and X_{21}^{de} of the impurity system, we make use of Eqs. (13a)–(13c), into which we make the following substitutions:

$$c(\mathbf{k}) = \begin{bmatrix} c_{11}(\mathbf{k}) & 0 \\ c_{21}(\mathbf{k}) & 1 \end{bmatrix}, \quad (26)$$

$$b(\mathbf{k}) = \begin{bmatrix} b_{11}(\mathbf{k}) & 0 \\ 0 & 1 \end{bmatrix}.$$

Then, using Eq. (13a), for example, N_{11}^{de} turns out to be

$$N_{11}^{de}(\mathbf{k}) = S_{11}(\mathbf{k})c_{11}(\mathbf{k})b_{11}(\mathbf{k})[1 - c_{11}(\mathbf{k})b_{11}(\mathbf{k})] + b_{11}(\mathbf{k}) - 1 - X_{11}^{de}(\mathbf{k}) + \{S_{21}(\mathbf{k})c_{21}(\mathbf{k})b_{11}(\mathbf{k})[1 - 2c_{11}(\mathbf{k})b_{11}(\mathbf{k})] - [c_{21}(\mathbf{k})b_{11}(\mathbf{k})]^2\}. \quad (27)$$

Now, $\rho_2 = \rho_1/N_1$, so that the term in the curly braces on the second line of Eq. (27) represents a contribution of order $1/N_1$ to the one-component quantity N_{11}^{de} because, according to our notation, the \mathbf{k} -space quantities contain the factor $(\rho_1\rho_2)^{1/2}$. This means that we can first solve the variational problem for the host system and then, separately, the following coupled FHNC equations for

the impurity:

$$N_{21}^{de}(\mathbf{k}) = S_{11}(\mathbf{k})[1 - c_{11}(\mathbf{k})b_{11}(\mathbf{k})] + c_{21}(\mathbf{k})[1 - b_{11}(\mathbf{k})], \quad (28)$$

$$X_{21}^{de}(\mathbf{r}) = \{g_{21}(\mathbf{r})/[1 + N_{21}^{de}(\mathbf{r})] - 1\}N_{21}^{de}(\mathbf{r}). \quad (29)$$

Note that $c_{21} = -X_{21}^{de}$. These two equations are the im-

purity FHNC equations to be solved for any given g_{21} and g_{11} . For Γ_{21}^{dd} and X_{21}^{dd} we obtain, from Eqs. (15) and (16),

$$\Gamma_{21}^{dd}(\mathbf{k}) = S_{21}(\mathbf{k})c_{11}(\mathbf{k})b_{11}(\mathbf{k}) + c_{21}(\mathbf{k})b_{11}(\mathbf{k}), \quad (30a)$$

$$X_{21}^{dd}(\mathbf{k}) = S_{21}(\mathbf{k})/S_{11}(\mathbf{k}) + c_{21}(\mathbf{k})c_{11}(\mathbf{k})b_{11}(\mathbf{k}), \quad (30b)$$

and again $N_{21}^{dd} = \Gamma_{21}^{dd} - X_{21}^{dd}$.

Next, the total energy of the impurity-host system has to be minimized with respect to g_{11} and g_{21} . Minimization with respect to g_{11} leads to the EL equations for the host system, since terms of order $1/N_1$ can be ignored. However, when calculating the immersion energy of the impurity, those contributions cannot be neglected. Instead, the immersion energy is calculated as

$$E_{21} = \delta E_{11} + \rho_1 \int d\mathbf{r} \left[[g_{21}(\mathbf{r}) - 1]v_{21}(\mathbf{r}) - \frac{\hbar^2}{8\mu_{21}} g_{21}(\mathbf{r}) \nabla^2 \{ \ln[1 + \Gamma_{21}^{dd}(\mathbf{r})] - N_{21}^{dd}(\mathbf{r}) \} \right], \quad (31)$$

where δE_{11} represents the $(1/N_1)$ -order effects in the correlation factor f_{11} of the host system. It amounts to

$$\delta E_{11} = \frac{\hbar^2}{8m_1} \rho_1 \int d\mathbf{r} [\{ 1/[1 + \Gamma_{11}^{dd}(\mathbf{r})] - 1 \} \delta \Gamma_{11}^{dd}(\mathbf{r}) - \delta X_{11}^{dd}(\mathbf{r}) \nabla^2 g_{11}(\mathbf{r}) - v_1 \delta \Gamma_{11}^{dd}(\mathbf{r}) [\nabla^2 L_{11}^2(\mathbf{r}) - 2N_{11}^{cc}(\mathbf{r}) \nabla^2 L_{11}(\mathbf{r})]], \quad (32)$$

where

$$\delta X_{11}^{dd}(\mathbf{k}) = -S_{21}^2(\mathbf{k})/S_{11}^2(\mathbf{k}), \quad (33)$$

$$\delta \Gamma_{11}^{dd}(\mathbf{k}) = 2S_{21}(\mathbf{k})c_{21}(\mathbf{k})c_{11}(\mathbf{k})b_{11}(\mathbf{k}) + [c_{21}(\mathbf{k})b_{11}(\mathbf{k})]^2. \quad (34)$$

Optimization of expression (31) with respect to g_{21} leads to the EL equation for the impurity-host correlation function. Again, we first consider the weakly interacting limit. We set $c_{21} = 0$, and retain only the leading term in the expansion of $\ln(1 + \Gamma_{21}^{dd})$; then, the energy becomes

$$E_{21} = \frac{1}{(2\pi)^3 \rho_1} \int d\mathbf{k} \left[S_{21}(\mathbf{k})v_{21}(\mathbf{k}) + \frac{\hbar^2 k^2}{8\mu_{21}} [S_{21}^2(\mathbf{k})/S_{11}(\mathbf{k})] \{ 1 - \mu_{21}[S_{21}(\mathbf{k}) - 1]/m_1 S_{11}(\mathbf{k}) \} \right]. \quad (35)$$

Minimization with respect to S_{21} (or g_{21}) leads to

$$S_{21}(\mathbf{k}) = \frac{4\mu_{21}}{\hbar^2 k^2} \frac{S_{11}^2(\mathbf{k})}{(\mu_{21}/m_1)[S_{11}(\mathbf{k}) - 1] - S_{11}(\mathbf{k})} v_{21}(\mathbf{k}). \quad (36)$$

If we now take the limit $m_2 \rightarrow \infty$ and identify the coefficient of $v_{21}(\mathbf{k})$ in Eq. (36) with the static linear-response function χ of the host system, as proposed by Kallio *et al.*,²¹ we get

$$\chi(\mathbf{k}) = -\frac{4m_1}{\hbar^2 k^2} S_{11}^2(\mathbf{k}). \quad (37)$$

This result is reasonable in the sense that it represents the response due to collective elementary excitations of the host fluid, i.e., plasmons or phonons which obey familiar Feynman dispersion relation

$$e(\mathbf{k}) = \frac{\hbar^2 k^2}{2m_1 S_{11}(\mathbf{k})}. \quad (38)$$

The approximate EL equation of the form (20) for a strongly interacting impurity is derived in a manner similar to that discussed in the preceding section [see Eq. (19)]. Now, the self-consistent induced potential to be used with Eq. (20) turns out to be

$$w_{21}(\mathbf{k}) = -\frac{\hbar^2 k^2}{4\mu_{21}} S_{21}(\mathbf{k}) \left[\frac{\mu_{21}}{m_1} \frac{S_{11}(\mathbf{k}) - 1}{S_{11}^2(\mathbf{k})} - \frac{1}{S_{11}(\mathbf{k})} + 1 \right]. \quad (39)$$

In deriving this equation we assumed that the energy terms proportional to c_{21} are small, so their variation can be ignored. Consequently, Eq. (39), which was earlier derived in Ref. 22, does not contain terms which explicitly depend on the fermion character of the host system. However, after solving the EL equation (20) with induced potential (39), we can use Eqs. (26) and (27) to obtain c_{21} , and then use the full energy expression (31) to compute the impurity energy.

We have applied this method to the case of a positron impurity in a host electron gas. Interesting quantities to be calculated are the immersion energy and the value of g_{21} at $\mathbf{r} = \mathbf{0}$. The latter allows us to compute the positron-annihilation rate in the electron fluid, which is given by

$$\lambda_p = \frac{12}{r_s^3} g_{21}(\mathbf{r} = \mathbf{0}) \times 10^9 \text{ s}^{-1}. \quad (40)$$

These results and an application of the multicomponent theory are discussed in the next section.

V. RESULTS AND DISCUSSION

As an application of this variational many-component FHNC theory, we have calculated correlation energies and pair distribution functions for a hypothetical electron-positron mixture. This two-component "jellium" is assumed to be neutralized by a properly charged rigid background, whenever the positron density is

smaller than that of electrons. Electronic densities are chosen to be in the metallic range, i.e., $r_s = 1-6$, and for each r_s , several values of positron concentration $x = \rho_2/\rho_1$ between 0 and 1 are considered. The $x = 0$ limit corresponds to a single positron in the electron gas and the fifty-fifty case $x = 1$ represents an ideal model for the electron-hole liquid (EHL). In the present case the mass ratio m_2/m_1 is set to unity, but we could have varied that too. However, we have not been able to solve the EL equations for very large mass ratios, corresponding to, for example, a proton-electron fluid (liquid metallic hydrogen).

The computational procedure for solving the many-component EL equations is based on linearization of Eqs. (20) and (21) and is similar to that developed earlier for the one-component system.^{19,20,5} To start, we need an initial guess for $g_{\alpha\beta}(r_j)$ ($j = 1, \dots, N$) in N mesh points on the r axis. Then we derive and solve a set of $3N$ linear equations for $\delta g_{\alpha\beta}(r_j)$, which represents corrections to initial g 's. The procedure is iterated several times until it converges. Naturally, the number of iterations depends greatly on the quality of the initial guess. It is possible, and often faster, to perform the iteration such that only one (or two) of the g 's is (are) varied at a time, while the remaining two (or one) are (is) kept fixed. Then the $g_{\alpha\beta}$ to be varied has to be alternated in some suitable manner. Doing this, one can avoid solving $3N$ simultaneous (linear) equations, and solve only N (or $2N$) of them. We wish to emphasize, however, that solving these EL equations is not any major numerical task. In the present study we have tabulated g 's (and other functions) in 55 mesh points, so that the size of largest matrix inverted was 165×165 . This yields reasonable numerical accuracy, keeping in mind other approximations made in deriving the equations and computing the energy.

After solving the EL equations for $g_{\alpha\beta}$, we proceed to solve the FHNC equations (13a)–(13c) and (8b)–(8d) using the solutions of the EL equations as input. This is done by direct iteration, without any linearization, starting with all the N 's set to zero. Usually, about 10–20 iterations are performed. At each step of iteration a new set of functions $X_{\alpha\beta}^i(\mathbf{r})$ is calculated using Eqs. (8b)–(8d); they are Fourier transformed and then inserted into Eqs. (13a)–(13c) to obtain a new set of $N_{\alpha\beta}^i(\mathbf{k})$. In this process “brute force” is exercised to make sure that each $X_{\alpha\beta}^{de}(\mathbf{k})$ goes to zero in the low-momentum limit. Namely, before inserting $X_{\alpha\beta}^{de}(\mathbf{k})$ into Eqs. (13a)–(13c), they are multiplied by a function which vanishes at $\mathbf{k} = \mathbf{0}$,

$$X_{\alpha\beta}^{de}(\mathbf{k}) \rightarrow [S_{F_\alpha}(\mathbf{k})S_{F_\beta}(\mathbf{k})]^{1/2} X_{\alpha\beta}^{de}(\mathbf{k}). \quad (41)$$

The vanishing of $X_{\alpha\beta}^{de}(\mathbf{k} \rightarrow \mathbf{0})$ is an exact property¹⁷ which is, unfortunately, violated by the FHNC approximation employed here. Similarly, $X_{\alpha\beta}^{ee}(\mathbf{k})$ should behave such that $1 + X_{\alpha\beta}^{ee}(\mathbf{k}) \rightarrow S_F(\mathbf{k})$ in the same limit, i.e.,

$$b(\mathbf{k} \rightarrow \mathbf{0}) = [S_F(\mathbf{k})]^{-1}, \quad (42)$$

but this was not forced to do so, because it did not seem

to be necessary and we wanted to avoid inconsistency between \mathbf{r} -space and \mathbf{k} -space quantities as much as possible. In the energy, the effect of imposing condition (41) remained small, but in some cases it crucially improved the convergence of the iteration of the FHNC equations.

Finally, the energy is calculated using expression (14). In order to make direct comparison of our results with those of the more familiar one-component electron gas, we have chosen to make use of normal electron-gas units, where the length scale is determined by the proton mass instead of the reduced mass of the electron-positron pair. Thus the length is measured in units of $r_s a_0$, where $a_0 = 0.523 \times 10^{-8}$ cm, $r_s = a_0 [3/(4\pi\rho_1)]^{1/3}$, and the energy unit is 1 Ry = 13.6 eV.

Since the induced potential was derived by making some simplifying approximations, we have tried to improve it by multiplying the fermion part of it, Eq. (23), by a constant λ , and then varied λ to obtain the lowest possible energy. In such a way we could lower the energy slightly. On the other hand, we have, just for simplicity, ignored a three-body term in the energy expression. When calculated, that term turn out to be positive, ranging from about 0.01 Ry at $r_s = 1$ to less than 0.001 Ry at $r_s = 5$, thus cancelling much of the energy gained by varying λ away from unity. Accordingly, we chose to use the induced potential of Eq. (23) as such and, at the same time, omitted the three-body term. Note that, in fact, we may manipulate the induced potential of the EL equation as we like. The best potential is the one which yields the lowest energy.

In recent variational work^{23–25} on a two-component fermion system, another form of the fermion (or exchange) part of the induced potential was used, which may be derived by employing other than the FHNC approximation to calculate the energy. That approximation, sometimes called the Lado approximation,²⁶ leads to

$$w_{\alpha\beta}^{ex}(\mathbf{r}) = -\delta_{\alpha\beta} \frac{\hbar^2}{4m_\alpha} \{2\nabla^2 u_\alpha^0(\mathbf{r}) + [\nabla u_\alpha^0(\mathbf{r})]^2\}. \quad (43)$$

Here, $u_\alpha^0(\mathbf{r})$ is determined to give the free-Fermi-gas pair distribution function g_F in boson HNC approximation, i.e.,

$$u_\alpha^0(\mathbf{r}) = \ln g_{F_\alpha}(\mathbf{r}) - N_\alpha^0(\mathbf{r}), \quad (44)$$

with

$$N_\alpha^0(\mathbf{k}) = [S_{F_\alpha}(\mathbf{k}) - 1]^2 / S_{F_\alpha}(\mathbf{k}). \quad (45)$$

In the case of one-component electron gas, this approximation yields solutions to the EL equations which are similar to those obtained by the present method or by the full optimization of the FHNC energy.²⁰ In a two-component plasma, however, a quite serious problem occurs when expression (43) is used. Namely, the EL equations become unstable for $r_s > 2$, in the sense that self-consistent solutions cannot be found by our iterative procedure. Physically, it is the antisymmetry of the wave function which prevents the two-component plasma from collapsing to very high density. In the EL

equation the antisymmetry shows up as the exchange part of the induced potential which is mainly repulsive. It seems that this Pauli repulsion is perhaps not adequately represented by Eq. (43). The main difference between the two approximations is that the exchange potential of Eq. (23) is more repulsive at small k than that of Eq. (43), leading to more stable EL equations. The instability shows up also when Eq. (23) is used, but at much lower density, namely near $r_s = 5$, which is clearly beyond the saturation density ($r_s \approx 4$).

For stable solutions the structure functions $S_{\alpha\beta}(\mathbf{k})$ vanish linearly as $\mathbf{k} \rightarrow 0$, unlike in the one-component plasma, in which they vanish quadratically. As we approach the region of the instability, the energy of the system become insensitive to the small variations of $g_{\alpha\beta}$ and the slopes of $S_{\alpha\beta}(\mathbf{k})$ seem to increase without limit. This may be taken as an indication that the system is close to the point of phase transition where the compressibility of the fluid diverges. If the exchange part of the induced potential is set to zero, the EL equations become unstable even at high density. This means that for the charged two-component boson system we do not find solutions of the EL equations at any density. Such a boson plasma would be always unstable against collapsing to infinitely high density.

We start discussing the results by showing, in Table I, correlation energies of the one-component jellium. This system has been very extensively studied by various methods. Presently its energy is believed to be known very accurately, thanks to the so-called Green's-function Monte Carlo calculation by Ceperley and Alder.²⁷ The results of the present work are quite close to those of Monte Carlo and some other works.^{28–31} This seems to be a good starting point for two-component computations. The fact that our present energies differ slightly from those obtained by more accurate optimization (Ref. 20) is partly due to imposing the ‘‘Fermi cancellation’’ constraint of Eq. (41), which introduces some inconsistency between r -space and k -space quantities. For example, Γ^{dd} calculated from Eq. (10) is not fully consistent with Eq. (15). In the present work we have used the expression (15) for Γ^{dd} in the energy integrations. This yields little smaller correlation energy than if Eq. (10) is used.

Vashista, Bhattacharyya, and Singwi³² (VBS) have, among others, studied the two-component mixtures of electrons and holes. For example, the question of whether electrons and holes form a bound liquid in stressed germanium has received much attention, both theoretically and experimentally. The results of VBS showed that almost certainly such a system would be bound. Recently, Chakraborty and Pietiläinen²⁴ (CP) published results, based on a variational approach, which were in apparent contradiction³³ with those of VBS. The difference in the results of those two works can be traced back to their treatment of the idealized system, i.e., the system equivalent to neutral electron-positron mixture. In Fig. 1 we compare the total energy of such an ideal system obtained by VBS, CP, and the present work. Note that the units of length and energy in the works of VBS and CP differ from ours by a factor of 2. Our result is in fairly good agreement with that of VBS and clearly much lower than that of CP. The energy calculation of CP employed the Lado approximation instead of the FHNC method used here. It seems, however, that most of the difference between our results and those of CP is due to the fact that the EL equations (20) do not have self-consistent solutions in the region of energy minimum, if the exchange part of the induced potential is taken to be that of Eq. (43). Due to some numerical reason, this instability did not show up in the work by CP, although the fact that the structure functions of CP did not vanish as $\mathbf{k} \rightarrow 0$ might have been taken as a hint of underlying problem. Rather peculiar small- k behavior of the partial structure functions occurred also when that method was applied to study the structure of liquid metallic hydrogen.²³ Curiously, with the present method we have not been able to solve the EL equations at all for very large mass ratios corresponding to metallic hydrogen.

Near the saturation density the Monte Carlo energies for the one-component fluid are slightly lower than those of the present work. This suggests that, if we add twice that difference into our two-component results, we end up with, hopefully, more accurate estimates for the true energy. Doing this, at $r_s = 4$, our energy is lowered by about 0.01 Ry to about -0.47 Ry, while the corresponding result of VBS is about -0.49 Ry. This amounts to

TABLE I. Correlation energy (Ry) in the one-component electron gas.

Method	$r_s =$	1	2	3	4	5
Present		-0.130	-0.090	-0.071	-0.059	-0.053
CA ^a		-0.120	-0.090	-0.074	-0.064	-0.056
VMC ^b		-0.122	-0.087	-0.072	-0.062	-0.055
BL ^c		-0.123	-0.086	-0.075	-0.064	-0.057
STLS ^d		-0.124	-0.092	-0.075	-0.064	-0.056
RPA ^e		-0.157	-0.124	-0.105	-0.094	-0.085
E ^f		-0.134	-0.094	-0.075	-0.064	-0.056

^aReference 27.

^bReference 28.

^cReference 29.

^dReference 30.

^eReference 31.

^fReference 1.

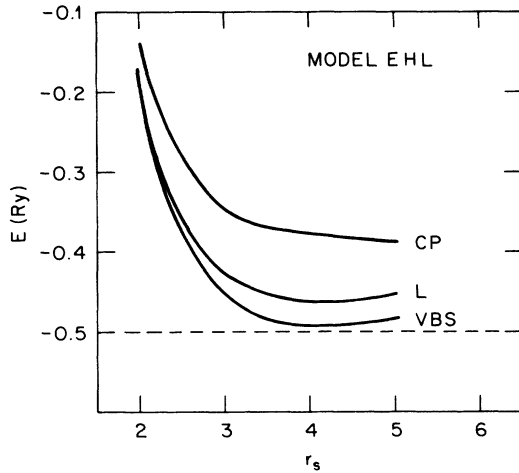


FIG. 1. Total energy of the model electron-hole liquid as a function of r_s . Curves labeled CP and VBS represent the results of Refs. 24 and 32, respectively, and the label L refers to the present work.

about 7% difference in the correlation energy, which is well within the uncertainty due to the approximations employed in the energy calculation of the present work. Whether the VBS energy is closer to the true energy is a question which may be answered only after accurate Monte Carlo calculations for this system are performed.

While our energy of the model system agrees quite well with that of VBS, the correlation functions of the two methods are very different. In Fig. 2 we show the partial pair-correlation functions g_{11} and g_{12} near the equilibrium density $r_s = 4$. The solid curves show the results of the present work and the dashed lines are reproduced from Figs. 4 and 5 of VBS. The oscillations in the g 's obtained by VBS are very much larger than what we have. For example, the minimum value of our $g_{12} - 1$ is about -0.05 , compared to about -0.35 in case of VBS. Similarly, the overshoot in the g 's of VBS is very large and in our case it is negligible. In this case we believe that it is fair to say that our results are physically more reasonable than those of VBS.

Values of $g_{12}(r=0)$ are given in Table II. Short-range behavior of our $g_{\alpha\beta}(r)$'s is very similar to that obtained by CP. As shown in Ref. 25, measured recombination rates in some EHL's compare favorably with predictions of the variational calculations. The results for the case $x = 0$ are obtained from the impurity calculations to be discussed below. From Table II we can see that the value of $g_{12}(0)$ is quite sensitive to the positron concen-

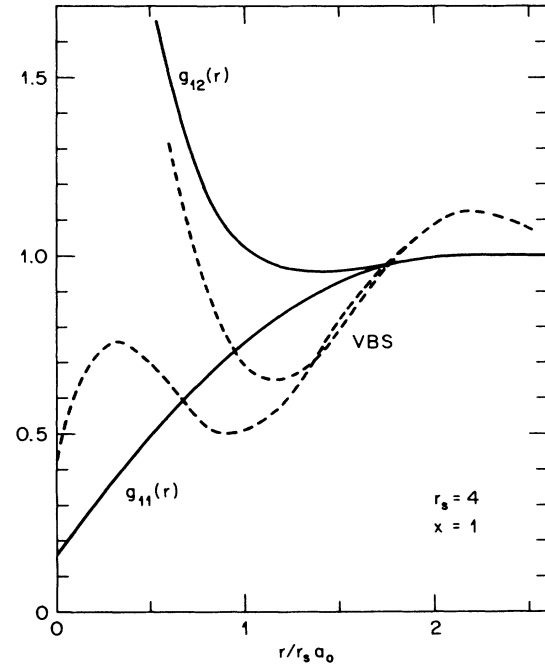


FIG. 2. The pair-correlation functions $g_{11}(r)$ and $g_{12}(r)$ for the model electron-hole liquid at $r_s = 4$. The solid lines show the results of the present work and the dashed lines represent results of Ref. 32 (VBS).

tration. It is obvious that the more we add positrons to electron gas the less there are electrons to screen each positron.

The static structure functions $S_{\alpha\beta}(\mathbf{k})$ for the positron-electron mixture at $r_s = 4$, $x = 0.125$ are shown by solid lines in Fig. 3. Clearly, they all vanish linearly as $\mathbf{k} \rightarrow 0$. $S_{12}(\mathbf{k})$ has a very strong $1/k^4$ tail as $k \rightarrow \infty$, corresponding to the strong peak at $g_{12}(r=0)$. The dashed lines in Fig. 3 represent corresponding ideal-gas structure functions. $S_{22}(\mathbf{k})$ deviates only slightly from the ideal-gas quantity. This is not so surprising if we realize that the positron-positron interaction is very efficiently screened by electrons. Electrons themselves are correlated more strongly, much like in the pure electron gas.

In Table III we show the correlation energy per electron $\epsilon(r_s, x)$ in the electron-positron mixture as a function of r_s and concentration x . Using these numbers we may calculate the "excess" electron-positron correlation energy per positron as

$$\epsilon_c^e(r_s, x) = [\epsilon(r_s, x) - \epsilon^1(r_s)] / x, \quad (46)$$

TABLE II. Values of $g_{12}(r=0)$ in positron-electron mixture as a function of electron density r_s and positron concentration x .

$x \setminus r_s =$	1	2	3	4	5
0.0	2.16	4.06	7.40	13.2	23.0
0.216	2.02	3.70	6.49	11.0	16.9
0.512	1.92	3.41	5.81	9.48	14.7
0.729	1.87	3.23	5.42	8.68	13.3
1.0	1.81	3.08	5.05	7.98	12.1

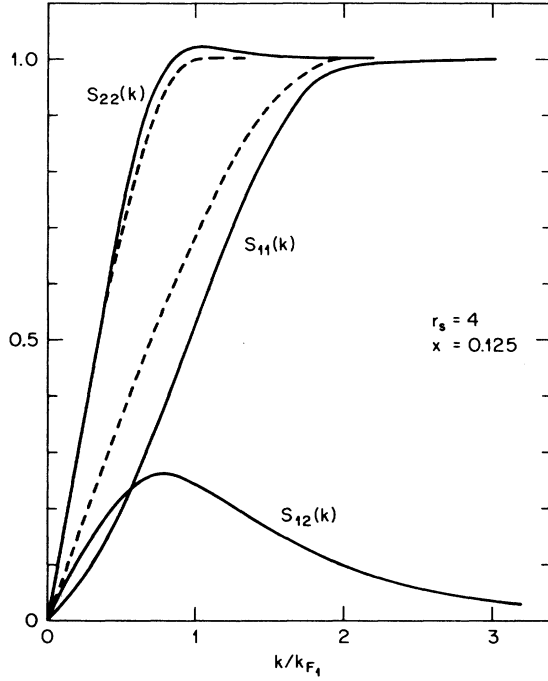


FIG. 3. Static structure functions $S_{11}(\mathbf{k})$, $S_{12}(\mathbf{k})$, and $S_{22}(\mathbf{k})$ for the positron-electron mixture for $r_s=4$, $x=0.125$ (solid lines) and corresponding ideal-gas structure functions (dashed lines).

where $\varepsilon^1(r_s)$ is the correlation energy of the one-component jellium. This excess energy per positron is shown in Fig. 4 for several values of x . In the limit $x \rightarrow 0$ this quantity becomes the energy of the positron impurity in the electron fluid. For comparison, the corresponding energy per electron in a pure one-component system is also shown. It is interesting to note that at small values of concentration the excess energy seems to be very sensitive to x . A word of caution is in order, however, since this quantity may be quite sensitive to the numerical accuracy of the two-component computation. There are three natural length scales in the problem, namely $r_s a_0$ for electron-electron correlations, $r_s a_0 / x^{1/3}$ for positron-positron correlations, and a_0 for electron-positron correlations. Admittedly, we did not try to compute the excess energy for small x very accurately because the limiting impurity energy is to be calculated

separately.

In order to get the impurity energy and the enhancement factor of the positron annihilation, we first solve EL equations (20) and (21) for the one-component host system. This gives us $g_{11}(\mathbf{r})$ and $S_{11}(\mathbf{k})$, which are then used to calculate the induced potential (39) for the impurity EL equation. That equation is easily solved and yields the impurity-host correlation function g_{21} . Next, the impurity FHNC equations (25) and (26) are used to obtain N_{21}^{de} , X_{21}^{de} , N_{21}^{dd} , and X_{21}^{dd} , which then allow us to compute the energy of the impurity particle with Eqs. (31) and (32). We note that now $S_{21}(\mathbf{k}) \rightarrow 1$ as $\mathbf{k} \rightarrow 0$, which reflects perfect screening of the charged impurity. Consequently, from Eqs. (25) and (26) we can see that N_{21}^{de} and X_{21}^{de} are not necessarily very small. It turns out that when g_{21} from the impurity EL equation is used as input to Eqs. (25) and (26), self-consistent solutions can be found only for small r_s . For increasing r_s , $g_{21}(\mathbf{r}=0)$ becomes very large and then $N_{21}^{de}(\mathbf{r}=0)$ approaches -1 , which causes $X_{21}^{de}(\mathbf{r}=0)$ to diverge. Presumably, this is an artifact of the FHNC approximation, which ignores elementary diagrams. Those diagrams may give a rather large contribution at small r because g_{21} is so large.

Because we were not able to solve the FHNC equations (25) and (26) consistently over the desired range of densities, and since the energy turned out to be quite sensitive to how X_{21}^{de} was approximated, especially for larger r_s , we decided to compute the impurity energy by setting $X_{21}^{de}=0$ for all r_s . This energy is shown in Fig. 4 by the curve labeled $x=0$, together with the result of Arponen and Pajanne³⁴ (AP), whose calculations are considered to be perhaps the most accurate ones available for this system. We can see that at small r_s the energies of the two very different methods agree quite well, and that for $r_s=4-5$ the difference between the two results is well within the uncertainty in our computation (due to setting $X_{21}^{de}=0$). Note that the induced potential (39) was derived under the assumption that $X_{21}^{de}=0$. This means that the fermion character of the host system shows up in the induced potential only via $S_{11}(\mathbf{k})$. In this approximation the impurity EL equation is exactly the same as that obtained in Ref. 22, but results for energy are different. In more accurate calculation we should include contributions proportional to X_{21}^{de} also in the derivation of the induced potential. It seems plausible, however, that those contributions remain small because our energies are not so far from those of AP. Of course, we have no way of knowing that the energies of

TABLE III. Total correlation energy in Ry per electron in the positron-electron mixture as a function of electron density r_s and positron concentration x .

$x \setminus r_s =$	1	2	3	4	5
0.0	-0.130	-0.090	-0.071	-0.059	-0.053
0.064	-0.163	-0.116	-0.095	-0.083	-0.078
0.125	-0.191	-0.139	-0.115	-0.102	-0.095
0.216	-0.227	-0.168	-0.141	-0.126	-0.119
0.343	-0.274	-0.205	-0.174	-0.157	-0.146
0.512	-0.331	-0.251	-0.214	-0.194	-0.181
0.729	-0.400	-0.300	-0.259	-0.234	-0.219
1.0	-0.466	-0.357	-0.308	-0.280	-0.262

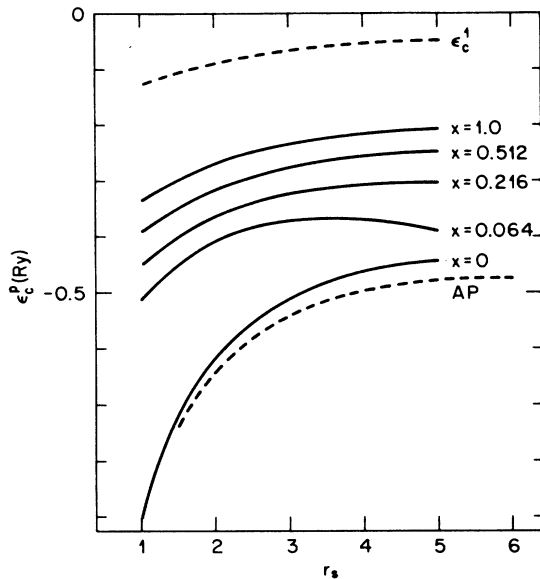


FIG. 4. Excess positron correlation energy per positron [see Eq. (46)] in the positron-electron mixture as a function of r_s for several values of positron concentration x . The curve marked $x=0$ shows the energy of a single positron impurity in an electron gas, and the curve labeled AP gives the corresponding result of Ref. 34. For comparison, the correlation energy of a one-component electron gas is also shown by the dashed line.

AP are indeed very close to the true energies, especially when the density is in the range $r_s=3-5$.

Finally, the positron-annihilation rate is determined, according to Eq. (40), by the value of the pair-correlation function g_{21} at the origin. Our results for the annihilation rate, which are shown in Fig. 5, are generally 10–15% lower than those of AP. In fact, this may be quite reasonable, since the rates obtained by AP tend to be slightly too large compared to experimental values. However, we cannot claim that the accuracy of our results for g_{21} is better than, say, 10%, although the present method is generally quite reliable in treating strong short-range correlations in various kinds of quan-

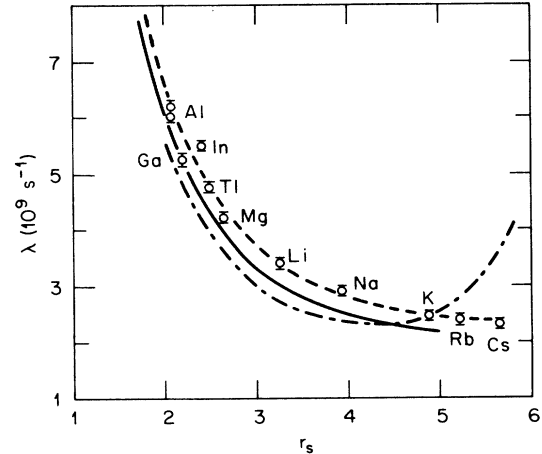


FIG. 5. Positron-annihilation rate in jellium as a function of r_s . The solid line shows the result of the present work. The dashed line (Ref. 34) and dotted-dashed line (Ref. 35) as well as experimental data are reproduced from Fig. 13 of Ref. 34.

tum fluids.

In conclusion, we have developed a simple variational theory for many-component quantum fluids, which makes use of multicomponent FHNC approximation and Euler-Lagrange equations in the calculation of the energy and static correlation functions of the system. Application to the case of a two-component plasma shows that the results obtained by this method are in good agreement with available experimental data and with the best theoretical calculations performed earlier.

ACKNOWLEDGMENTS

The author wishes to thank Dr. T. Chakraborty, Professor A. Kallio, and Dr. P. Pietiläinen for collaboration and stimulating discussions during the early part of this work. This work was supported by the Finnish Academy of Science, by the National Science Foundation under Grant No. PHY-86-8418, and by the U.S. Department of Energy through Contract No. DE-AS05-76ER0-4936 with the Joint Institute for Heavy Ion Research at Oak Ridge National Laboratory.

*On leave from Department of Theoretical Physics, University of Oulu, SF-90570 Oulu, Finland.

¹E. Krotscheck, *Ann. Phys. (N.Y.)* **155**, 1 (1984), and references therein.

²A. Manousakis, S. Fantoni, V. R. Pandharipande, and Q. N. Usmani, *Phys. Rev. B* **28**, 3770 (1983), and references therein.

³V. R. Pandharipande and R. B. Wiringa, *Rev. Mod. Phys.* **51**, 821 (1979), and references therein.

⁴A. Fabrocini and A. Polls, *Phys. Rev. B* **25**, 4533 (1982).

⁵Tapash Chakraborty, *Phys. Rev. B* **25**, 3177 (1982).

⁶K. E. Kürten and C. E. Campbell, *Phys. Rev. B* **26**, 124 (1982).

⁷M. Saarela, P. Pietiläinen, and A. Kallio, *Phys. Rev. B* **27**, 231 (1983).

⁸E. Krotscheck, W. Kohn, and Guo-Xin Qian, *Phys. Rev. B* **32**, 5693 (1985).

⁹A. D. Jackson, A. Lande, and R. A. Smith, *Phys. Rep.* **86**, 55 (1982).

¹⁰T. M. Rice, in *Solid State Physics*, edited by F. Seitz and D. Turnbull (Academic, New York, 1977), Vol. 32, p. 1.

¹¹E. Boronski and R. M. Nieminen, *Phys. Rev. B* **34**, 3820 (1986).

¹²S. Fantoni and S. Rosati, *Nuovo Cimento A* **25**, 593 (1975).

¹³E. Krotscheck and M. L. Ristig, *Nucl. Phys. A* **242**, 389 (1975).

¹⁴J. W. Clark, in *Progress in Nuclear and Particle Physics*, edited by D. H. Wilkinson (Pergamon, Oxford, 1979), Vol. 2, p. 89.

¹⁵G. Ripka, *Phys. Rep.* **56**, 1 (1979).

- ¹⁶S. Fantoni and S. Rosati, *Phys. Lett.* **84B**, 23 (1979).
¹⁷E. Krotscheck, *Nucl. Phys.* **A317**, 149 (1979).
¹⁸L. J. Lantto, A. D. Jackson, and P. J. Siemens, *Phys. Lett.* **68B**, 311 (1977).
¹⁹L. Lantto and P. J. Siemens, *Nucl. Phys.* **A317**, 55 (1979).
²⁰L. J. Lantto, *Phys. Rev. B* **22**, 1380 (1980).
²¹A. Kallio, P. Pietiläinen, and L. Lantto, *Phys. Scr.* **25**, 943 (1982).
²²P. Pietiläinen and A. Kallio, *Phys. Rev. A* **27**, 224 (1983).
²³T. Chakraborty, A. Kallio, L. J. Lantto, and P. Pietiläinen, *Phys. Rev. B* **27**, 3061 (1983).
²⁴Tapash Chakraborty and P. Pietiläinen, *Phys. Rev. Lett.* **49**, 1034 (1982).
²⁵Tapash Chakraborty, *Phys. Rev. B* **29**, 3975 (1984).
²⁶J. G. Zabolitzky, *Phys. Rev. B* **22**, 2353 (1980).
²⁷D. M. Ceperley and B. J. Alder, *Phys. Rev. Lett.* **45**, 566 (1980); S. H. Vosko, L. Wilk, and M. Nusair, *Can. J. Phys.* **58**, 1200 (1980).
²⁸D. Ceperley, *Phys. Rev. B* **18**, 3126 (1978).
²⁹R. F. Bishop and K. H. Lührmann, *Phys. Rev. B* **26**, 5523 (1982).
³⁰K. S. Singwi, M. P. Tosi, R. H. Land, and A. Sjölander, *Phys. Rev.* **176**, 589 (1968).
³¹D. Pines and P. Nozierès, *Theory of Quantum Fluids* (Benjamin, New York, 1966).
³²P. Vashista, P. Bhattacharyya, and K. S. Singwi, *Phys. Rev. B* **10**, 5108 (1974).
³³P. Vashista, R. K. Kalia, and K. S. Singwi, *Phys. Rev. Lett.* **50**, 2036 (1983); Tapash Chakraborty and P. Pietiläinen, *ibid.* **50**, 20 (1983).
³⁴J. Arponen and E. Pajanne, *Ann. Phys. (N.Y.)* **121**, 343 (1979).
³⁵A. Sjölander and M. J. Stott, *Phys. Rev. B* **5**, 2109 (1972).